β-Delayed α Spectrum of ^{16}N and the $^{12}C(\alpha,\gamma)^{16}O$ Cross Section at Low Energies

L. Buchmann,[1] R. E. Azuma,[2] C. A. Barnes,[3] J. M. D'Auria,[4] M. Dombsky,[4,5] U. Giesen,[1,2] K. P. Jackson,[1,4] J. D. King,[2] R. G. Korteling,[4] P. McNeely,[5] J. Powell,[2] G. Roy,[5] J. Vincent,[1] T. R. Wang,[2,3] S. S. M. Wong,[2] and P. R. Wrean[3]

[1] *TRIUMF, Vancouver, British Columbia, Canada V6T 2A3*

[2] *University of Toronto, Toronto, Ontario, Canada M5S 1A7*

[3] *W.K. Kellogg Laboratory, California Institute of Technology, Pasadena, California 91125*

[4] *Simon Fraser University, Burnaby, British Columbia, Canada V5A 1S6*

[5] *University of Alberta, Edmonton, Alberta, Canada T6G 2J1*

(Received 3 November 1992)

The α spectrum following the β decay of ^{16}N from the isotope separator TISOL has been measured by detecting 10^6 α particles in coincidence with ^{12}C nuclei. These data, which show a low-energy interference anomaly accompanying the main α peak, permit a more precise determination of the p-wave amplitude of the astrophysically important reaction $^{12}C(\alpha,\gamma)^{16}O$. The α spectrum and previous γ-ray data have been fitted simultaneously by a K-matrix parametrization; a value of $S(E = 0.3$ MeV$) = 57 \pm 13$ keV b has been obtained for the $E1$ part of the $^{12}C(\alpha,\gamma)^{16}O$ reaction.

PACS numbers: 23.60.+e, 25.55.Ci, 27.20.+n, 95.30.Cq

Because of its crucial role in stellar evolution calculations, there has been, for many years, a great deal of interest in the low-energy cross section of the radiative capture reaction $^{12}C(\alpha,\gamma)^{16}O$ [1–6]. The $E1$ and $E2$ components of this cross section at stellar helium-burning energies ($E_{c.m.} \simeq 0.3$ MeV) are dominated by the tails of the $J^\pi = 1^-$ and $J^\pi = 2^+$ subthreshold resonances corresponding to the bound states at 7.12 and 6.92 MeV, respectively [7]. However, the cross section in the experimentally accessible region above $E_{c.m.} \sim 1$ MeV is dominated by the resonance corresponding to the 1^- state at $E_x = 9.6$ MeV for p-wave ($E1$) capture, and by direct capture for the d wave ($E2$).

Several studies [4, 5, 8], using both R- and K-matrix fits, have attempted to extrapolate the cross section down to $E_{c.m.} = 0.3$ MeV using the available $^{12}C(\alpha,\gamma)^{16}O$ and $^{12}C(\alpha,\alpha)^{12}C$ data sets. These calculations yield large uncertainties dominated by the errors in the fitted values of the reduced α-particle widths of the subthreshold states.

Other work [9–14] has, in addition, incorporated the α-particle spectrum following β decay of ^{16}N in an attempt to improve the reliability of the extrapolation. Two factors enhance the ^{16}N β decay to the region of ^{16}O near the α-decay threshold—the favorable $\log ft$ value to the subthreshold 7.12-MeV state [7] and the β-decay phase space. This strongly increases the influence of this state on the shape of the α-particle spectrum, producing a destructive interference anomaly in the spectrum for energies $E_{c.m.} < 1.5$ MeV [12–14]. In addition to selecting the p-wave part of the interaction, the $^{16}N(\beta,\alpha)^{12}C$ decay permits an f-wave contribution to the α-particle spectrum from allowed β decay to $J^\pi = 3^-$ states in ^{16}O.

The only high-statistics, published spectrum of α particles associated with ^{16}N β decay has a low-energy cutoff at $E_\alpha \simeq 1.08$ MeV (E_α is the α-particle energy measured in the laboratory) and requires correction for electron counts up to 1.3 MeV [15]. In this Letter we report a new measurement of the α-particle spectrum extending down to 0.63 MeV.

Proton beams up to 2 μA at 500 MeV, from the TRIUMF Cyclotron, were used to bombard a 13.1-g/cm^2 zeolite target which formed part of the TISOL isotope separator [16–18]. A 12-keV, mass-30 beam containing $^{16}N^{14}N^+$ molecular ions was focused through an 8-mm collimator and implanted in thin (10 μg/cm^2) self-supporting carbon collector foils of 1 cm diameter. Liquid-nitrogen-cooled surfaces close to the collector foil minimized carbon buildup. Four such foils were mounted on a wheel perpendicular to the beam direction, with one foil located at the collection point and the other three positioned between pairs of Si surface-barrier detectors (separation $\simeq 5$ mm, area = 50 mm^2). After a 3-s implantation time, the wheel was rotated through 90° in 0.25 s, transferring the collected ^{16}N ($t_{\frac{1}{2}}$=7.1 s) to a position between the first pair of detectors. The intensity of the radioactive beam at the foil was typically (0.5–1) $\times 10^6$ ^{16}N ions/s.

Thin detectors, ranging in thickness from 10.6 to 15.8 μm, were chosen to minimize the effects of the β particles whose intensity is 10^5 times that of the α particles. The preamplifier output from each detector was further amplified with a shaping time of 3 μs and sent to an analog-to-digital convertor (ADC). All ADC's were read out upon receipt in any channel of a signal corresponding to $E_\alpha > 0.25$ MeV. Thus, in addition to singles, coincidences were also recorded even for events where the ^{12}C pulse height was substantially lower than this value.

The energy scale of the α-particle detectors was cal-

ibrated with the known [19, 20] monoenergetic decay lines of the $\beta\alpha$ decay of ^{18}N [1.083 ± 0.004 MeV and 1.409±0.003 MeV (laboratory), respectively]. The width of these peaks ($\Delta E \approx 45$ keV FWHM) provides an upper limit on the energy resolution of the detector system. (The ^{18}N peaks are broadened by β and ν recoil effects.)

The energy ratio of the α and the ^{12}C particles in the ^{16}O breakup should be 3. However, the maximum of the peak in the pulse-height-ratio spectrum is between 4 and 5. This is due primarily to the larger pulse-height defects in the detection of the ^{12}C particles, and to the larger stopping power for ^{12}C particles in the gold entrance layer of the detectors (40 μg/cm^2) and in the collector foils.

Figure 1 shows a two-dimensional contour plot of the energies of α and ^{12}C particles in coincidence. Events with an energy ratio of $E_1/E_2 \approx 4.5/1$ or $1/4.5$ are seen as intense diagonal bands. The two bands extending horizontally or vertically at about 0.45 MeV from the intense main peaks to low energies are coincidence events for which the α particles have been degraded in energy (in either the detector or the collector foil) whereas the ^{12}C particles have not. These energy-degraded events constitute the tail of the response function of the detector. With appropriate cuts during data analysis, the "tail" events (which were ~0.7%–1.0% of the total) can be excluded from the coincidence spectra.

The relative coincidence efficiency was determined to be constant within 0.5% down to an effective α energy of 1.08 MeV by comparing singles and coincidence spectra for the ^{18}N $\beta\alpha$ decay and for the main peak in the ^{16}N $\beta\alpha$ decay. The calculation was extended down to $E_\alpha = 0.75$ MeV (where the ^{12}C counts begin to appear in the singles spectrum) by adding tail events back into the coincidence spectrum. The ratio of events was found to be constant within ±3%, indicating no change of coincidence efficiency. No direct measurement of the coincidence efficiency was possible below $E_\alpha = 0.75$ MeV, but extensive Monte Carlo calculations indicate that the efficiency remains constant down to $E_\alpha = 0.63$ MeV.

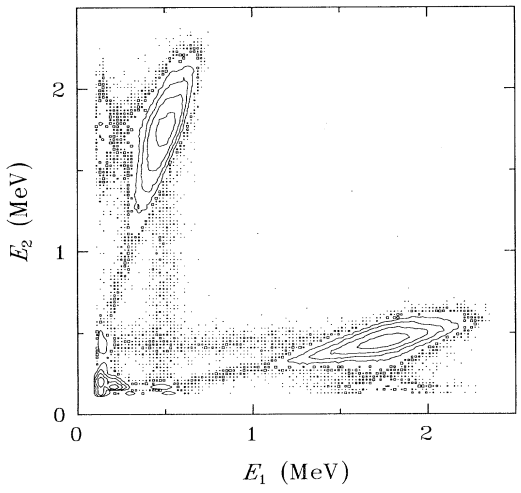

FIG. 1. Contour plot of particles in coincidence. The energy calibration is for α particles. Contour lines are shown for 30, 100, 300, and 1000 counts and the minimum displayed intensity is 1 count.

Pileup effects were observed as a high-energy tail on the pulser peak. These tails are of the order of a few tenths of a percent for our thin detectors, decreasing exponentially by about 1 order of magnitude per two channels (about 4 keV).

Contamination from ^{18}N ($t_{\frac{1}{2}} = 0.62$ s) and ^{17}N ($t_{\frac{1}{2}} = 4.2$ s) was observed in the spectra. Because of its short half-life, the ^{18}N appeared in significant amounts only in the first set of detectors and could be easily subtracted. A weak $\beta\alpha$ decay of ^{17}N has been observed for the first time in our laboratory [21]. To determine the amount of ^{17}N in the beam, Ge(Li) observations of the characteristic γ decays of $^{16-18}$N were made and the number of α particles resulting from the $\beta\alpha$ decay of ^{17}N calculated and subtracted. The total yield from ^{17}N and ^{18}N is less than 0.3% of the α yield obtained from ^{16}N.

The corrected α-particle coincidence spectrum summed over all six detectors is shown in Fig. 2(a).

In K-matrix theory, the β-delayed α-particle spectrum of ^{16}N can be fitted by the expression [12]

$$W_{\ell\alpha}(E) = f_\beta(E)\, p^2_{\ell\alpha}(E) \left| \frac{\sum_i \frac{B_{\ell i}\, g_{\ell\alpha i}}{E_{\ell i} - E}}{1 - i p^2_{\ell\alpha}(E) K_{\ell\alpha\alpha}} \right|^2 \qquad (1)$$

and the $E1$ part of the ^{12}C$(\alpha,\gamma)\,^{16}$O cross section can be fitted by

$$\sigma_{E1} = \frac{12\pi}{k^2} p^2_{1\alpha} p^2_{1\gamma} \left| \frac{b_{1\alpha\gamma} + \sum_i \frac{g_{1\gamma i}\, g_{1\alpha i}}{E_{1i} - E}}{1 - i\, p^2_{1\alpha} K_{1\alpha\alpha}} \right|^2 , \qquad (2)$$

where the subscript ℓ refers to the angular momentum of the decay (here ℓ=1 or 3 for the p or f wave, respectively); $f_\beta(E)$ is the integrated Fermi distribution; $p^2_{\ell c}(E)$ is the K-matrix penetrability for channel c; $E_{\ell i}$ is the energy of the state i; $g_{\ell ci}$ is the K-matrix partial width of state i for channel c; $B_{\ell i}$ is the β-feeding factor into state i; $K_{\ell\alpha\alpha}$ is given by

$$K_{\ell\alpha\alpha} = b_{\ell\alpha\alpha} + \sum_i \frac{g^2_{\ell\alpha i}}{E_{\ell i} - E}; \qquad (3)$$

$b_{\ell\alpha\alpha}$ and $b_{1\alpha\gamma}$ are constant background terms; and k is the wave number.

It is customary to express the cross section in terms of the astrophysical S factor,

$$S(E) = E \exp(2\pi\eta)\, \sigma(E), \qquad (4)$$

where E is the c.m. energy and η is the Sommerfeld parameter.

In the fitting of these expressions to the experimental data, we followed the procedures and parametrizations of Ref. [12]. In addition, Eq. (1) was convo-

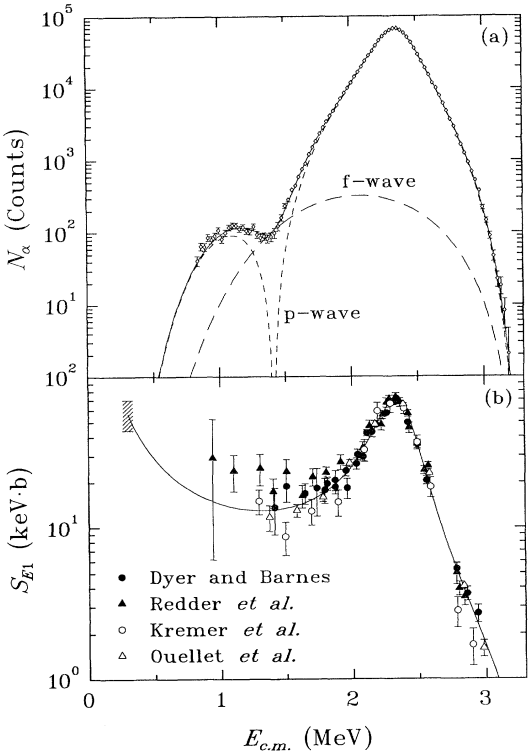

FIG. 2. (a) The α-particle spectrum with ^{17}N and ^{18}N background subtracted. The best K-matrix fit with the use of the entire (α,γ) data set is shown including the separate p and f waves. (b) The S factor for the $^{12}C(\alpha,\gamma)^{16}O$ reaction fitted with the present data and all the radiative capture data. The cross-hatched line at 0.3 MeV indicates the range of $S_{E1}(0.3)$ values allowed by the present fit.

TABLE I. Best-fit K-matrix parameters for background state energies E_{13} set at 7 and 20 MeV (using a = 5.46 fm [12]).

	E_{13} = 7 MeV	E_{13} = 20 MeV
E_{11} (MeV)	$(-0.0451)^a$	(-0.0451)
B_{11}	$(1198)^b$	$(1198)^b$
$g_{1\gamma1}a^{-3/2}$ (MeV$^{1/2}$)	$(1.897\times10^{-3})^c$	$(1.897\times10^{-3})^c$
$g_{1\alpha1}a^{-3/2}$ (MeV$^{1/2}$)	-5.612	-6.226
E_{12} (MeV)	2.414	2.402
B_{12}	-375.3	-365.1
$g_{1\gamma2}a^{-3/2}$ (MeV$^{1/2}$)	6.287×10^{-4}	6.208×10^{-4}
$g_{1\alpha2}a^{-3/2}$ (MeV$^{1/2}$)	6.604	6.550
E_{13} (MeV)	(7.000)	(20.00)
B_{13}	-642.8^d	$-1756i^d$
$g_{1\gamma3}a^{-3/2}$ (MeV$^{1/2}$)	$-1.039\times10^{-3\,d}$	$-1.071\times10^{-2}i^d$
$g_{1\alpha3}a^{-3/2}$ (MeV$^{1/2}$)	18.55^d	$-28.75i^d$
$b_{1\alpha\alpha}a^{-3}$	-1.519	136.0
$b_{1\alpha\gamma}a^{-3}$	5.021×10^{-3}	1.764×10^{-2}
E_{31} (MeV)	(-1.032)	(-1.032)
B_{31}	$(4388)^b$	$(4388)^b$
$g_{3\alpha1}a^{-7/2}$ (MeV$^{1/2}$)	3.628×10^{-2}	3.553×10^{-2}
$S_{E1}(0.3)$ (keV b)	57 ± 13^e	68 ± 14^e
$\chi^2_{^{16}N}$ (89 points)	130	116
$\chi^2_{\alpha,\gamma}$ (71 points)	194	191

[a]Terms in parentheses are fixed.
[b]B_{11} and B_{31} fixed from branching ratios.
[c]From $\Gamma_{1\gamma}$ = 55 meV.
[d]Best fit with real or echo pole, excluding elastic data.
[e]Total error (see text).

luted with the detector resolution before fitting to the α-particle spectrum. In Ref. [12], data from three reactions [$^{16}N(\beta,\alpha)^{12}C$ [15], $^{12}C(\alpha,\gamma)^{16}O$ [3–5], and $^{12}C(\alpha,\alpha)^{12}C$ [22–24]] were included in the overall fits. However, we note that the inclusion of the elastic scattering data leads to a poor fit and to systematic differences in the width and energy of the 9.6 MeV state of ^{16}O. Therefore the scattering data were not included in our final fits.

Following Ref. [12], we used a background state plus a constant background term, as well as the 7.12 and 9.6 MeV states, in the fit to the p wave and a single state in the fit to the f wave. The ^{16}N coincidence data were fitted simultaneously with all of the radiative capture data sets [3–6] to determine the value for $S_{E1}(0.3)$. Table I lists the K-matrix parameters for background state energies set to 7 and 20 MeV. The coefficients $g_{\ell\alpha\alpha}$ are related to the reduced width in the R-matrix formulation. Figure 2(a) shows the results of the fit for the α spectrum with the background state set to 7 MeV. Figure 2(b) shows the corresponding fit to the entire $^{12}C(\alpha,\gamma)^{16}O$ data set [3–6].

The statistical error assigned to each fit was one-half the change in $S_{E1}(0.3)$ given by an increase of 4.0 in the value of the total χ^2. With B_{11} fixed (see below), the statistical error is ±2 keV b.

Systematic errors include uncertainties in the energy calibration, dependence of the coincidence efficiency on the α energy, uncertainty in TISOL beam contaminants, and energy dependence of the detector resolution. The ^{16}N spectrum has been varied and fitted to incorporate these uncertainties as systematic errors. Our best estimate of the systematic error is ±5 keV b.

Another source of uncertainty in the fits is the 10% error in the β-decay feeding factor B_{11} of the 7.12 MeV state in the ^{16}N decay [12]. Varying B_{11} within its experimental uncertainty produced a change of ±8 keV b in $S_{E1}(0.3)$.

Because of the wide disparity between the different capture results, a contribution to the error in $S_{E1}(0.3)$ was determined by fitting the ^{16}N data with each of the (α,γ) data sets separately. The standard deviation of these four values was used to assign an uncertainty of ±8 keV b (±10 keV b, E_{13}=20 MeV). The average value from the separate fits is in good agreement with the value

from the simultaneous fit.

Fits to the singles spectra, corrected for the response function, yield a consistent result. The higher low-energy cutoff in the singles data has little influence on the S factor. A more detailed discussion of this experiment, including the use of the different data sets and fitting procedures, is in preparation [25].

The S factor at 0.3 MeV for $E1$ α capture by ^{12}C is then

$$S_{E1}(0.3) = 57 \pm 13\,\text{keV b} \quad (5)$$

for the background state fixed at 7 MeV. We have assumed that the various errors given above are not correlated and have added them in quadrature to produce the quoted error. The S factor increases somewhat if a higher background state energy is used (Table I). The present $S_{E1}(0.3)$ is considerably lower than that derived in Ref. [4]; it is within the errors, though somewhat lower, than that in Ref. [3]; it is close to the values given in Ref. [5]; and it is considerably larger than the value given in Ref. [6].

The inclusion of the improved data for the α-particle spectrum following β decay of ^{16}N in a simultaneous fit with the radiative capture data has significantly reduced the uncertainty in $S_{E1}(0.3)$ for the $^{12}\text{C}(\alpha,\gamma)^{16}\text{O}$ reaction. Substantially improved experimental data are now required for the $E2$ part of the $^{12}\text{C}(\alpha,\gamma)^{16}\text{O}$ cross section to reduce the large uncertainty in $S_{E2}(0.3)$.

We wish to thank H. Biegenzein, D. Jones, P. Machule, H. Sprenger, A. Wilson, and G. Sheffer for help with the technical aspects of the experiment, and D. Diel and P. W. Green for assistance with the data acquisition system. Our special thanks goes to Teleglobe Canada for the donation of a 6 GHz amplifier without which the operation of the ECR source at TISOL and this experiment would have been impossible. The help of A. Chen, J. Chen, and M. Trinczek is gratefully acknowledged. One of the authors (R.E.A.) wishes to express his thanks to the Kellogg Radiation Laboratory at Caltech for their hospitality during the early stages of the experiment. This work was supported in part by TRIUMF, by the Natural Sciences and Engineering Research Council of Canada, and by the National Science Foundation (Grant No. PHY-91-15574).

[1] W.A. Fowler, Rev. Mod. Phys. **56**, 149 (1984).
[2] T.A. Weaver and S.E. Woosley, Phys. Rep. (to be published).
[3] P. Dyer and C.A. Barnes, Nucl. Phys. **A233**, 495 (1974).
[4] A. Redder, H.W. Becker, C. Rolfs, H.P. Trautvetter, T.R. Donoghue, T.C. Rinckel, J.W. Hammer, and K. Langanke, Nucl. Phys. **A462**, 385 (1987).
[5] R.M. Kremer, C.A. Barnes, K.H. Chang, H.C. Evans, B.W. Filippone, K.H. Hahn, and L.W. Mitchell, Phys. Rev. Lett. **60**, 1475 (1988).
[6] J.M.L. Ouellet, H.C. Evans, H.W. Lee, J.R. Leslie, J.D. MacArthur, W. McLatchie, H.-B. Mak, P. Skensved, J.L. Whitton, X. Zhao, and T.K. Alexander, Phys. Rev. Lett. **69**, 1896 (1992).
[7] F. Ajzenberg-Selove, Nucl. Phys. **A460**, 1 (1986).
[8] B.W. Filippone, J. Humblet, and K. Langanke, Phys. Rev. C **40**, 515 (1989).
[9] F.C. Barker, Aust. J. Phys. **24**, 777 (1971).
[10] F.C. Barker, Aust. J. Phys. **40**, 25 (1987).
[11] F.C. Barker and T. Kajino, Aust. J. Phys. **44**, 369 (1991).
[12] J. Humblet, B.W. Filippone, and S.E. Koonin, Phys. Rev. C **44**, 2530 (1991).
[13] X. Ji, B.W. Filippone, J. Humblet, and S.E. Koonin, Phys. Rev. C **41**, 1736 (1990).
[14] D. Baye and P. Descouvemont, Nucl. Phys. **A481**, 445 (1988).
[15] K. Neubeck, H. Schober, and H. Wäffler, Phys. Rev. C **10**, 320 (1974); H. Hättig, K. Hünchen, and H. Wäffler, Phys. Rev. Lett. **25**, 941 (1970).
[16] M. Dombsky, J.M. D'Auria, L. Buchmann, H. Sprenger, J. Vincent, P. McNeely, and G. Roy, Nucl. Instrum. Methods Phys. Res., Sect. A **295**, 291 (1990).
[17] L. Buchmann, J. Vincent, H. Sprenger, M. Dombsky, J.M. D'Auria, P. McNeely, and G. Roy, Nucl. Instrum. Methods Phys. Res., Sect. B **62**, 521 (1992).
[18] M. Dombsky, L. Buchmann, J.M. D'Auria, P. McNeely, G. Roy, H. Sprenger, and J. Vincent, Nucl. Instrum. Methods Phys. Res., Sect. B **70**, 125 (1992).
[19] F. Ajzenberg-Selove, Nucl. Phys. **A475**, 1 (1988).
[20] Z. Zhao, M. Gai, B. Lund, S.L. Rugari, D. Mikolas, B.A. Brown, J.A. Nolen, and M. Samuel, Phys. Rev. C **39**, 1985 (1989).
[21] M. Dombsky, R.E. Azuma, L. Buchmann, J.M. D'Auria, U. Giesen, K.P. Jackson, J.D. King, E.Korkmaz, R.G. Korteling, P. McNeely, J. Powell, G. Roy, J. Vincent, and S.S.M. Wong (to be published).
[22] C. Miller Jones, G.C. Phillips, R.W. Harris, and E.H. Beckner, Nucl. Phys. **37**, 1 (1962).
[23] G.J. Clark, D.J. Sullivan, and P.B. Treacy, Nucl. Phys. **A110**, 481 (1968).
[24] R. Plaga, H.W. Becker, A. Redder, C. Rolfs, H.P. Trautvetter, and K. Langanke, Nucl. Phys. **A465**, 291 (1987).
[25] R.E. Azuma, L. Buchmann, C.A. Barnes, J.M. D'Auria, M. Dombsky, U. Giesen, K.P. Jackson, J.D. King, R.G. Korteling, P. McNeely, J. Powell, G. Roy, J. Vincent, P.R. Wrean, and S.S.M. Wong (to be published).